



# Experimental Thermal Performance Of A Stirling Machine Milli-Regenerator Made By Multiple Jet Molding

Emna Dellali, François Lanzetta, Sylvie Bégot, Eric Gavignet, Jean-Yves Rauch

## ► To cite this version:

Emna Dellali, François Lanzetta, Sylvie Bégot, Eric Gavignet, Jean-Yves Rauch. Experimental Thermal Performance Of A Stirling Machine Milli-Regenerator Made By Multiple Jet Molding. International Conference on Heat Transfer, Fluid Mechanics and Thermodynamics, Jul 2021, Amsterdam, Netherlands. hal-03359931

**HAL Id: hal-03359931**

**<https://hal.science/hal-03359931>**

Submitted on 30 Sep 2021

**HAL** is a multi-disciplinary open access archive for the deposit and dissemination of scientific research documents, whether they are published or not. The documents may come from teaching and research institutions in France or abroad, or from public or private research centers.

L'archive ouverte pluridisciplinaire **HAL**, est destinée au dépôt et à la diffusion de documents scientifiques de niveau recherche, publiés ou non, émanant des établissements d'enseignement et de recherche français ou étrangers, des laboratoires publics ou privés.

# EXPERIMENTAL THERMAL PERFORMANCE OF A STIRLING MACHINE MILLI-REGENERATOR MADE BY MULTIPLE JET MOLDING

Dellali E.<sup>1</sup>, Lanzetta F.\*<sup>1</sup>, Bégot S.<sup>1</sup>, Gavignet E.<sup>1</sup> and Rauch J.Y.<sup>2</sup>

\* Author for correspondence

FEMTO-ST Institute, Univ. Bourgogne Franche-Comté, CNRS

<sup>1</sup> Energy Department, Parc technologique, 2 avenue Jean Moulin, 90000 Belfort, France

<sup>2</sup> AS2M Department (ENSMM), 26 rue de l'Épitaphe, 25000 Besançon, France

E-mail: francois.lanzetta@univ-fcomte.fr

## ABSTRACT

This paper focuses on the thermal performances of a regenerator with millimeter dimensions. This specific heat exchanger plays a crucial role in Stirling cycle machines. The considered milli-regenerator is a porous medium fabricated with a Multiple Jet Molding (MJP). We have quantified the pumping power required to convey the fluid in the circuit for an alternating oscillating flow and shown that this power is dependent on the piston strokes that induce more pressure losses in the hydraulic circuit. Calculation of the thermal efficiencies of the regenerator during the "cold-blow" and "hot-blow" phases showed that the thermal efficiency decreases as a function of the Reynolds number. An estimation of the figure of merit showed an increasing overall trend in the report pressure drop and heat transfer within the regenerator according to an increasing Reynolds number of flow. This can be explained by the nature of the regenerator of polymer of relatively low thermal diffusivity which limits the thermal performance of the regenerator, especially for high frequencies and consequently reduced exchange times. We demonstrated that the increase in the area-to-volume ratio at small scales increases pressure drop and enhances the heat transfer.

## INTRODUCTION

This paper focuses on the thermal performances of a regenerator with millimetre dimensions. This specific heat exchanger plays a crucial role in Stirling cycle machines. It alternately absorbs and releases heat from and to the working fluid which allows to recycle rejected heat during theoretical isochoric processes.

We have quantified the pumping power required to convey the fluid in the circuit for an alternating oscillating flow and shown that this power is dependent on the piston strokes that induce more pressure losses in the hydraulic circuit. Calculation of the thermal efficiencies of the regenerator during the "cold-blow" and "hot-blow" phases showed that the thermal efficiency decreases as a function of the Reynolds number. An estimation of the figure of merit showed an increasing overall trend in the report pressure drop and heat transfer within the regenerator according to an increasing Reynolds number of flow. This can be

## NOMENCLATURE

$A$	[m <sup>2</sup> ]	Section area
$cp$	[J/kg/K]	specific heat
$C$	[m]	Stroke
$CB$	[-]	Cold Blow
$C_f$	[-]	Friction factor
$CHEx$	[-]	Cold Heat EXchanger
$D$	[m]	Diameter
$E$	[-]	Efficiency
$HHEX$	[-]	Hot Heat EXchanger
$f$	[Hz]	Frequency
$F$	[-]	Form factor
$F_M$	[-]	Figure of Merit
$h$	[m]	Height
$\bar{h}$	[W/m <sup>2</sup> /K]	Mean value of convection coefficient
$HB$	[-]	Hot Blow
$L$	[m]	Length
$\dot{m}$	[kg/s]	mass flow
$NPH$	[-]	Net Pressure Head
$NUT$	[-]	Number of Unit Transfer
$Nu$	[-]	Nusselt number
$Pr$	[-]	Prandtl number

### Special characters

$\alpha$	[-]	Volume fraction ratio
$\epsilon$	[-]	Porosity
$\Delta$	[-]	Difference
$\rho$	[m <sup>3</sup> /kg]	Density

### Subscripts

$c$	cold
$HEX$	heat exchanger
$f$	fluid
$h$	hot

explained by the nature of the regenerator which is made of polymer of relatively low thermal diffusivity, which limits the thermal performance of the regenerator, especially for frequencies and consequently reduced exchange times. We demonstrated that the increase in the area-to-volume ratio at small scales increases pressure drop and enhances the heat transfer.

## EXPERIMENTAL SETUP

### Regenerator fabrication

The considered milli-regenerator is a porous medium fabricated with a Multiple Jet Molding (MJP) process by the use of the 3D printer ProJet HD 3500. The material used for the preparation of the regenerator is a UV-curable acrylate polymer of the type "Visijet 39 Crystal". The mini-regenerator is a tube with

and a total length  $L = 60\text{mm}$  and an external diameter  $D = 7\text{mm}$ , an internal diameter  $D = 5\text{mm}$  filled with a dense pillar matrix Figure 1. The pillars have a geometrical lens shape with a form factor  $F = 0.5$  (aspect ratio width/length) and a height  $h = 2.5\text{mm}$  (Figure 1b). Two metallic layers (chromium and copper) with a total thickness of 800 nm are deposited on the polymer pillars to increase heat transfer inside the regenerator (Figure 1c). Experiments were performed with three regenerator porosities:  $\epsilon = 0.8$ ; 0.85 and 0.90.

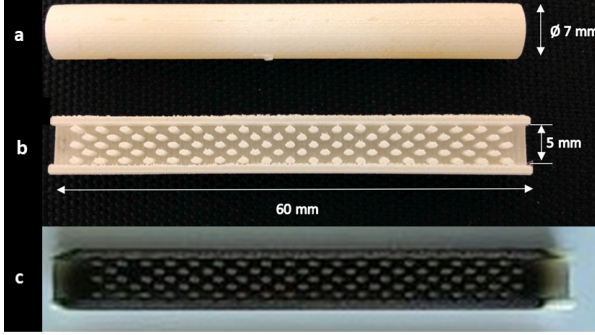


Figure 1: Regenerator fabricated.  $\epsilon = 0.8$ , a) Outside view, b) Sectional view, c) Polymer pillars with metallic layers

### Experimental procedure

Experiments are carried out with air as working gas. The oscillating gas flow is produced by the displacement of two connected pistons with a phase shift of  $180^\circ$  (Figure 2). Two heat exchangers heat (HHEX) and cool (CHEX) the gas flow at both ends of the measurement section. The regenerator is mounted between the two heat exchangers. The pressure, velocity and temperature of the airflow are measured in the spaces between the heat exchangers and the extremities of the regenerator. Metallic grids are included at both ends to smooth the turbulence of the flow.

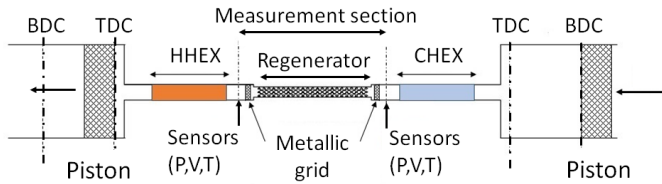


Figure 2: Experimental setup

The exchangers are temperature-controlled and keep a temperature gradient between the two ends of the regenerator of  $\Delta T = 30^\circ\text{C}$ ,  $40^\circ\text{C}$  and  $50^\circ\text{C}$ . The strokes of the pistons are  $C = 24\text{mm}$  and  $C = 30\text{mm}$ .

The pressure, velocity and temperature of the gas flow are measured at both ends of the test section. The ultraminiature pressure transducers are Kulite XCQ-055 1.7 BARA-8068, with 210 kHz bandwidth. They were calibrated using a Druck PV621 Pressure Station. The velocity measurement is achieved with a hot wire

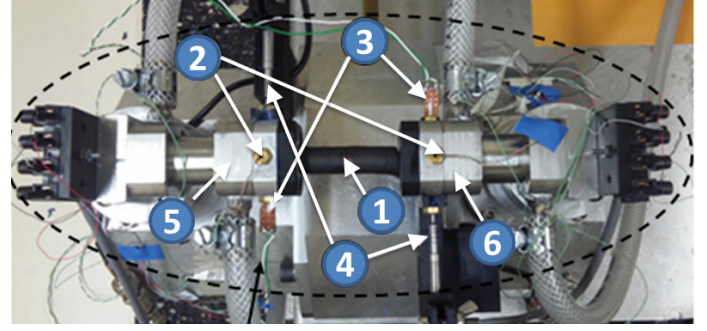


Figure 3: Test bench - ①: Regenerator, ②: Pressure sensor, ③: Microthermocouple, ④: Hot wire, ⑤: Hot Heat Exchanger HHEX, ⑥: Cold Heat Exchanger CHEX

anemometry method (TSI IFA300 range 0.15–200 m/s, 600 kHz bandwidth). The probe measures the axial velocity component and was calibrated in the laboratory. The fluid temperatures are measured with in-house  $0.76\text{ }\mu\text{m}$  diameter type K microthermocouples with accuracy  $\pm 0.1^\circ\text{C}$  and cut-off frequency 32 Hz (Figure 4) [5]. All the temperature sensors were calibrated using a calibration oven (550 Gemini LRI) associated with a Pt100 platinum reference sensor (accuracy  $\pm 0.005^\circ\text{C}$ ) and a reference thermometer (PHP 601). Measurements data were smoothed with a Savitzky-Golay filter [6].

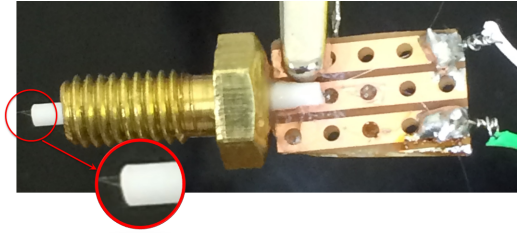


Figure 4: Microthermocouple (K type,  $7.6\text{ }\mu\text{m}$  diameter) inserted in a screw

We conducted experiments with regenerators of three porosities ( $\epsilon = 0.80$ , 0.85 and 0.90). These tests were made for five frequencies: 2, 4, 6, 8 and 10 Hz.

We performed experiments on different milli-regenerators with pillar geometries corresponding to three porosities under oscillating nitrogen flows (oscillating Reynolds number in the range  $0 < Re_\omega < 60$  and Reynolds number based on the hydraulic diameter  $Re_{Dh,max} < 6000$ ) for different temperature gradients ( $\Delta T < 100^\circ\text{C}$ ).

Figures 5 to 7 show the results of data acquisition for pressure, temperature and fluid velocity measured at both ends of the regenerator. From these data, we determined the pressure losses and friction coefficients [2]. In this paper, we will focus on the thermal characteristics of this type of flow: the thermal efficiency and the figure of merit of the regenerator.

### Uncertainty analysis

An uncertainty analysis need to be performed in order to identify the sources of errors concerning the different velocities, pres-

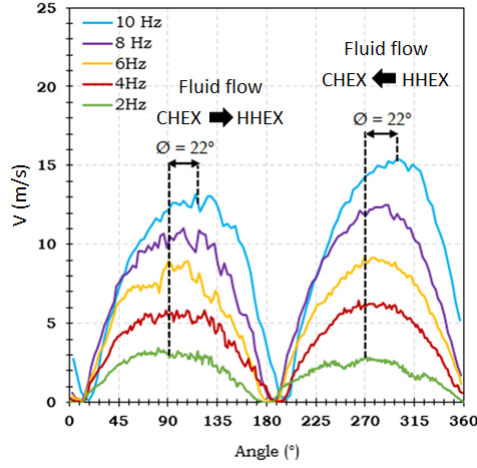


Figure 5: Gas velocity at the hot outlet of the regenerator ( $\epsilon = 0.8$ ,  $C = 30$  mm, Isothermal flow  $22^\circ\text{C}$ )

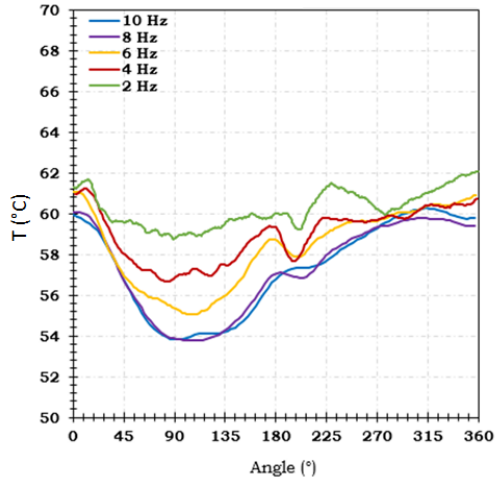


Figure 6: Temperature of the gas at the hot outlet of the regenerator ( $\epsilon = 0.8$ ,  $C = 30$  mm)

Table 1: Total relative uncertainties

	Total relative uncertainty	
Frequency $f$	2 Hz	10 Hz
Pressure $P$	5.7 %	3.9 %
Velocity $V$	3.7 %	2.4 %
Temperature $T$	$0.1^\circ\text{C}$	$0.2^\circ\text{C}$

tures and temperatures measurements. The total relative uncertainties are given in the table 1 [1], [3].

## RESULTS ANALYSIS

### Thermal efficiency

We will study the thermal efficiency for different regenerator porosities and piston strokes. The cold-blow and hot-

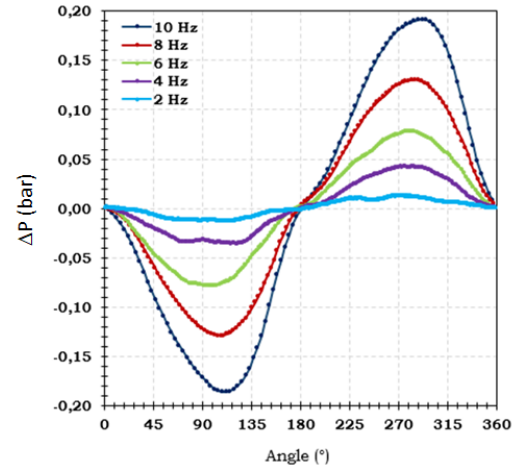


Figure 7: Pressure losses of the regenerator fluid flow ( $\epsilon = 0.8$ ,  $C = 30$  mm, Isothermal flow  $22^\circ\text{C}$ )

blow phases of the cycle present dissymmetries (Figure 5). We have chosen to calculate the corresponding efficiencies for each phase. The regenerator is assimilated to a heat exchanger whose efficiency is calculated from the temperatures of the incoming/outgoing fluid during a "period blow" which corresponds to a piston stroke (passage from TDC to BDC and vice versa). For the cold-blow, the thermal efficiency  $E^+$  can be written as follow:

$$E^+ = \frac{\min(T_{hot,CB}) - \min(T_{cold,CB})}{T_{HHEX} - \min(T_{cold,CB})} \quad (1)$$

and for the hot-blow,  $E^-$  yields:

$$E^- = \frac{\max(T_{cold,HB}) - \max(T_{hot,HB})}{T_{CHEX} - \max(T_{hot,HB})} \quad (2)$$

These two equations (1) and (2) are written in terms of the different temperatures:

- $T_{hot,CB}$ : temperature of the fluid at the hot end of the regenerator during cold-blow;
- $T_{cold,CB}$ : temperature of the fluid at the cold end of the regenerator during cold-blow;
- $T_{HHEX}$ : mean temperature of the fluid inside the hot heat exchanger
- $T_{cold,HB}$ : temperature of the fluid at the cold end of the regenerator during hot-blow;
- $T_{hot,HB}$ : temperature of the fluid at the hot end of the regenerator during hot-blow;
- $T_{CHEX}$ : mean temperature of the fluid inside the cold heat exchanger.

The frequency Reynolds number  $Re_\omega$  allows us to decouple the effect of frequency from that of fluid displacement, which

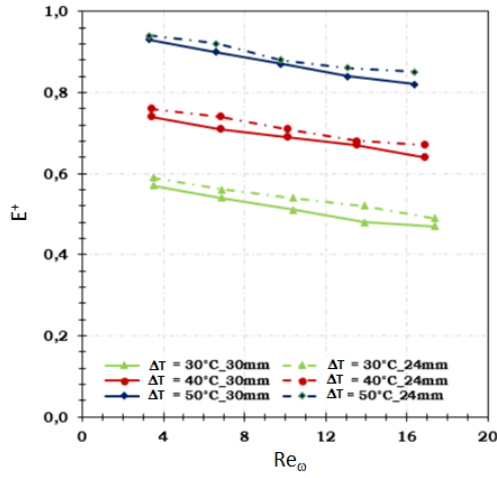


Figure 8: Variation of the thermal efficiency of the regenerator  $E^+$  during cold-blow with piston stroke  $C = 24$  mm, porosity  $\epsilon = 0.8$ , as a function of the frequency Reynolds number  $Re_\omega$  and temperature differences  $\Delta T = 30^\circ\text{C}$ ,  $40^\circ\text{C}$  and  $50^\circ\text{C}$

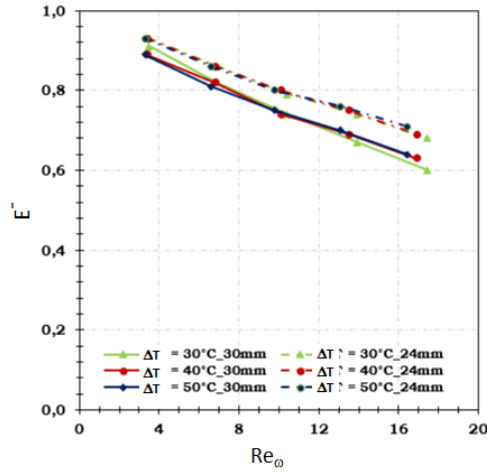


Figure 9: Variation of the thermal efficiency of the regenerator  $E^-$  during hold-blow with piston stroke  $C = 30$  mm, porosity  $\epsilon = 0.8$ , as a function of the frequency Reynolds number  $Re_\omega$  and temperature differences  $\Delta T = 30^\circ\text{C}$ ,  $40^\circ\text{C}$  and  $50^\circ\text{C}$

are coupled in the expression for the Reynolds number  $Re_{Dh}$ , and thus to be able to study only the effect of oscillations in the flow on the the flow on the thermal efficiency of the regenerator (Figure 8). We note that the thermal efficiency decreases for an increasing frequency Reynolds number  $Re_\omega$  increasing, which is to be expected since the frequencies are higher and the time of exchange between fluid and solid matrix is reduced. We show that for each temperature gradient, the thermal efficiency increases by 10% when the stroke increases from 24 mm to 30 mm. The thermal efficiency depends on the heat transfer coefficient and the flow rate through the regenerator. The heat transfer coefficient is improved in the presence of turbulence in the flow inherent to

high flow rates which implies higher Reynolds numbers. Higher flow rates mean that for the same power stored in the same power stored in the solid matrix, the heating of the fluid will be less important. It is a question of finding a compromise between heat transfer and fluid flow rates through the regenerator. For that we introduce the number of transfer units  $NUT$  which is written:

$$NUT = \frac{\bar{h}A_{HEX}}{\dot{m}c_{p_f}} \quad (3)$$

For a lower stroke, for the same flow frequency, the mass flow rate decreases, the thermal efficiency is lower. The efficiency of the heat exchanger increases as a function of the thermal gradient imposed on the ends of the regenerator, which is quite predictable.

The thermal efficiency is lower for the for the largest stroke  $C = 30$  mm (Figure 9). The effect of the thermal gradient on the variation of the efficiency is less obvious since the curves are close to each other.

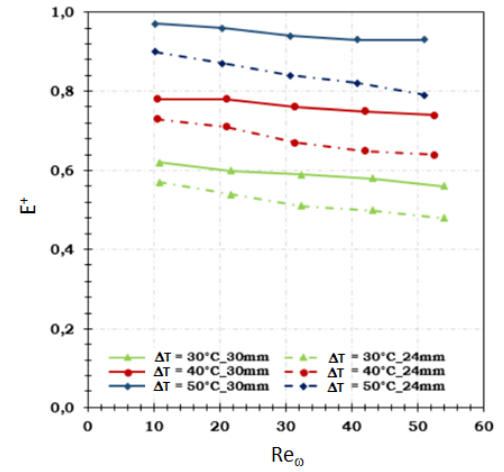


Figure 10: Variation of the thermal efficiency of the regenerator  $E^+$  during cold-blow with piston stroke  $C = 30$  mm, porosity  $\epsilon = 0.9$ , as a function of the frequency Reynolds number  $Re_\omega$  and temperature differences  $\Delta T = 30^\circ\text{C}$ ,  $40^\circ\text{C}$  and  $50^\circ\text{C}$

Figure 10 shows the same decay trend as a function of the frequency Reynolds number  $Re_\omega$ . In this case study, the thermal efficiency increases for a larger stroke in the opposite of what we have previously observed for the porosities  $\epsilon = 0.80$  and  $\epsilon = 0.85$ . This inversion can be explained by the nature of the flow which remains transient and generates turbulences. Figure 11, which describes the evolution of the thermal efficiency of the regenerator of porosity  $\epsilon = 0.90$  during the hot-blow, shows that the effect of the thermal gradient remains less pronounced than in the cold-blow.



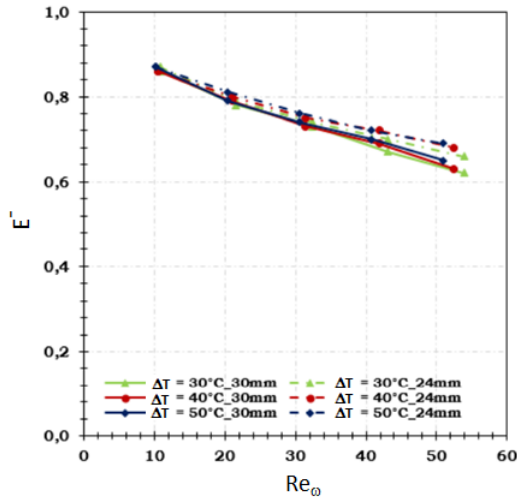


Figure 11: Variation of the thermal efficiency of the regenerator  $E^-$  during hot-blow with piston stroke  $C = 30$  mm, porosity  $\varepsilon = 0.90$ , as a function of the frequency Reynolds number  $Re_\omega$  and temperature differences  $\Delta T = 30^\circ\text{C}$ ,  $40^\circ\text{C}$  and  $50^\circ\text{C}$

#### Figure of Merit ( $F_M$ )

The figure of merit  $F_M$  quantifies the heat transfers in relation to the pressure losses within the regenerator. We used the criterion proposed by [7]:

$$F_M = \frac{NPH}{NTU} = \frac{C_f Re_{Dh} Pr}{4 \bar{Nu}} \quad (4)$$

Rülich and Quack [7] have established equation (4) for a permanent and unidirectional flow. We will use this method by considering the hot-blow and the cold-blow phases separately for the calculation of the regenerator figure of merit. As the flow is oscillating, we considered the maximum values of the pressure drop coefficient and the hydraulic Reynolds number,  $C_{f,max}$  and  $Re_{Dh,max}$  respectively. To get the average Nusselt number over a cycle  $\bar{Nu}$ , we have estimated the convective coefficient  $\bar{h}$  from the expression relating the  $NTU$  and the regenerator efficiency  $E$  [4], [8].

$$E = \frac{NTU}{1 + NTU} \quad (5)$$

Figures 12 and 13 show the figure of merit  $F_M$  for a thermal gradient equal to  $\Delta T = 50^\circ\text{C}$  for a piston stroke  $C = 30$  mm during the cold-blow and hot-blow phases respectively. It can be seen that during the cold-blow (Figure 12) the figure of merit tends to increase for higher Reynolds numbers, especially for porosities  $\varepsilon = 0.80$  and  $\varepsilon = 0.85$ , which means that the ratio between pressure drop and heat transfer increases as a function of the Reynolds number, this trend is less clear for  $\varepsilon = 0.90$  which shows a dip marking the beginning of a growth. This trend is

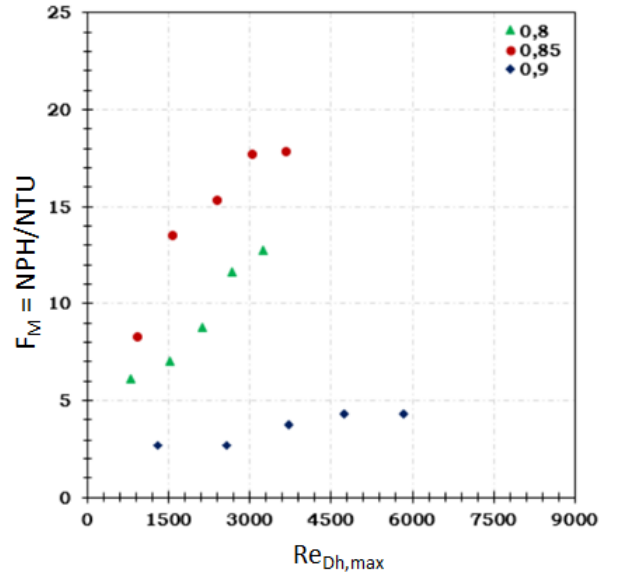


Figure 12: Variation of the thermal efficiency of the regenerator during cold blow with porosity as a function of the frequency Reynolds number  $Re_\omega$ , ( $\varepsilon = 0.80$ ,  $C = 24$  mm and  $C = 30$  mm,  $\Delta T = 30^\circ\text{C}$ ,  $40^\circ\text{C}$  and  $50^\circ\text{C}$ )

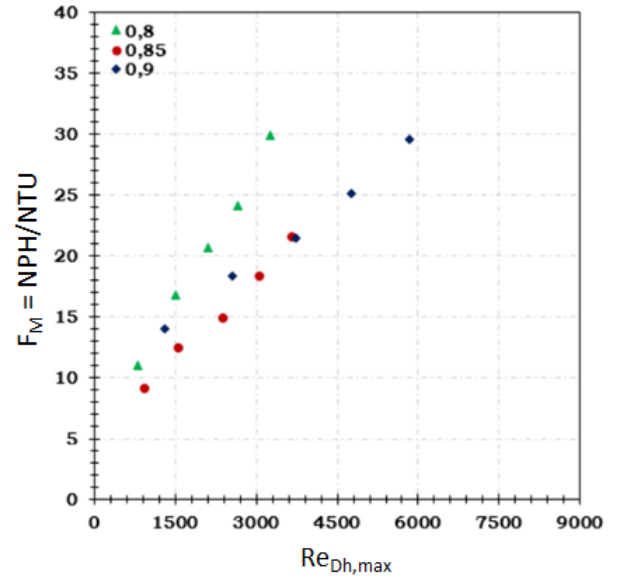


Figure 13: Variation of the thermal efficiency of the regenerator during hot-blow with porosity as a function of the frequency Reynolds number  $Re_\omega$ , ( $\varepsilon = 0.80$ ,  $C = 24$  mm and  $C = 30$  mm,  $\Delta T = 30^\circ\text{C}$ ,  $40^\circ\text{C}$  and  $50^\circ\text{C}$ )

confirmed during the hot-blow phase, where the  $(\frac{NPH}{NTU})$  ratio increases as a function of the Reynolds number, which means that pressure losses are more important than heat transfers. During the hot-blow phase, the increase trend is located in the same envelope for the three thermal gradients imposed, unlike the cold-blow phase for which the envelope shifts towards higher values for a decreasing thermal gradient (Figures 12, 13 and 14). This

can be explained by the decreasing thermal efficiency of the regenerator at lower thermal gradients and the pressure drop is not influenced by the thermal gradient

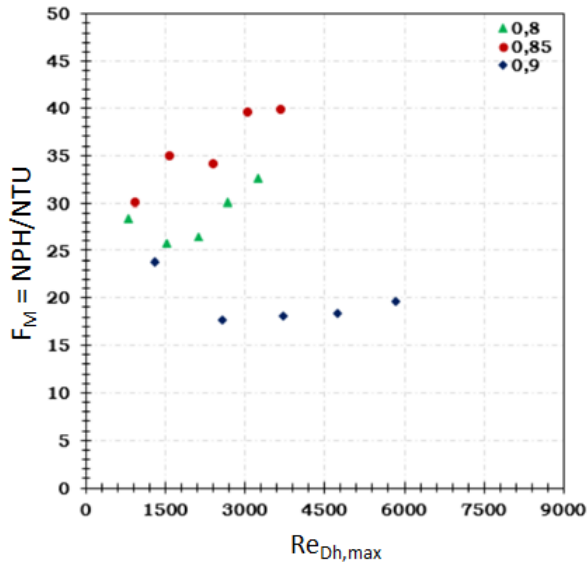


Figure 14: Variation of the thermal efficiency of the regenerator during cold-blow with porosity as a function of the frequency Reynolds number  $Re_\omega$  ( $\epsilon = 0.80$ ,  $C = 24$  mm and  $C = 30$  mm,  $\Delta T = 30^\circ C, 40^\circ C$  and  $50^\circ C$ )

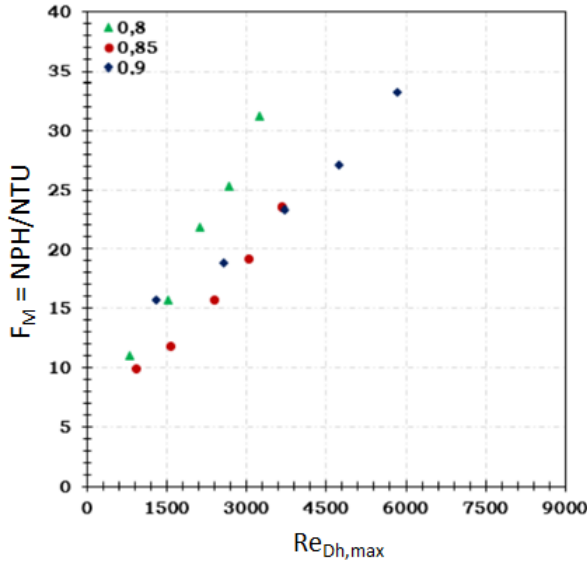


Figure 15: Variation of the thermal efficiency of the regenerator during hot-blow with porosity as a function of the frequency Reynolds number  $Re_\omega$  ( $\epsilon = 0.80$ ,  $C = 24$  mm and  $C = 30$  mm,  $\Delta T = 30^\circ C, 40^\circ C$  and  $50^\circ C$ )

## CONCLUSION

Calculations of the thermal efficiencies of the regenerator during the cold-blow and hot-blow phases showed that the thermal efficiency decreases as a function of the Reynolds number of the flow, but the effect of porosity could not be established from the experimental results. An estimation of the figure of merit  $F_M$  showed an overall increasing trend in the ratio of pressure drop and heat transfer within the regenerator with increasing Reynolds number of the flow. This can be explained by the nature of the regenerator, which is made of a polymer with relatively low thermal diffusivity, which limits the thermal performance of the regenerator, especially for higher frequencies and consequently longer running times. This limits the thermal performance of the regenerator, particularly at higher frequencies and consequently at shorter exchange times.

## ACKNOWLEDGMENT

This work has been supported by the EIPHI Graduate School (contract "ANR-17-EURE-0002").

## References

- [1] E. Dellali. "Étude théorique et expérimentale des écoulements oscillants alternés d'un gaz au sein de micro et milli-régénérateurs de moteur Stirling". PhD thesis. Univ. Bourgogne Franche-Comté, 2018.
- [2] Emna Dellali et al. "Pressure drop analysis of oscillating flows through a miniature porous regenerator under isothermal and nonisothermal conditions". In: *Experimental Thermal and Fluid Science* 103 (2019), pp. 394–405. DOI: <https://doi.org/10.1016/j.expthermflusci.2019.01.027>.
- [3] GUM. *Evaluation of measurement data — Guide to the expression of uncertainty in measurement*. Tech. rep. JCGM - Joint Committee for Guides in Metrology, 2008. URL: <https://www.iso.org/sites/JCGM/JCGM-introduction.htm>.
- [4] William Morrow Kays and Alexander Louis London. *Compact heat exchangers*. McGraw-Hill, New York, NY, 1984.
- [5] François Lanzetta and Eric Gagnier. "Temperature Measurements: Thermoelectricity and Microthermocouples". In: *Thermal Measurements and Inverse Techniques* (2011), p. 95.
- [6] William H Press and Saul A Teukolsky. "Savitzky-Golay smoothing filters". In: *Computers in Physics* 4.6 (1990), pp. 669–672.
- [7] I Rühlich and H Quack. "Investigations on regenerative heat exchangers". In: *Cryocoolers 10*. Springer, 2002, pp. 265–274.
- [8] Koji Yanaga, Ruijie Li, and Songgang Qiu. "Robust foil regenerator flow loss and heat transfer tests under oscillating flow condition". In: *Applied Thermal Engineering* 178 (2020), p. 115525.